Oncology
and Radiotherapy©
18 (1) 2024: 001-008 • RESEARCH ARTICLE

Design, synthesis, and evaluation of activity against breast cancer cells of new naphthalene derivatives as potential sirtuin enzymes inhibitors

Yahya Mohammed, Ayad A. Al-Hamashi

Department of Pharmaceutical Chemistry, College of Pharmacy, University of Baghdad, Baghdad, Iraq

ABSTRACT

Epigenetic modifications are potentially therapeutic targets because of their reversibility in somatic inheritability patterns. The sirtuin enzyme family is a Nicotinamide Adenine Dinucleotide (NAD+)-dependent histone deacetylase. Sirtuins have been associated with the pathogenesis of cancer due to their function in gene expression, making them an interesting therapeutic target. In the current study, several naphthalene-containing molecules were designed. The molecular docking Glide software from Schrodinger Inc. was used to evaluate the virtual interactions of the designed compounds with sirtuin enzymes. Compounds with acceptable docking scores were nominated for organic synthesis. The new naphthalene derivatives were synthesized and characterized via FTIR and NMR spectroscopy. A preliminary antiproliferative study over aggressive, poorly differentiated, and multi-treatment resistant triple negative receptor breast cancer cells (AMJ13) showed that compound Y4 has a significant cytotoxicity with an IC50 of 82.8 M, which was comparable to the vorinostat with an IC50 of 85.9 M. The ADMET study indicated that compound Y4 has acceptable pharmacokinetic properties and a drug-like profile.

Keywords: breast cancer, molecular docking, naphthalene, sirtuins

Address for correspondence:
Yahya Mohammed, Department of Pharmaceutical Chemistry, College of Pharmacy, University of Baghdad, Baghdad, Iraq; E-mail: ph.ym1992@gmail.com

Word count: 3955 **Tables:** 04 **Figures:** 06 **References:** 38

Received: 12 November, 2023, Manuscript No. OAR-23-119885

Editor: 18 November, 2023, Pre-QC No. OAR-23-119885 (PQ)

Reviewed: 03 December, 2023, QC No. OAR-23-119885 (Q)

Revised: 10 January, 2024, Manuscript No. OAR-23-119885 (R)

Published: 15 February, 2024, Invoice No. J-119885

INTRODUCTION

Cancer is the world's second-most common cause of death, involving about 277 distinct forms [1]. Epigenetics is the study of heritable changes in gene expression without DNA sequence changes. Recent investigations demonstrate that epigenetic mechanism modifications play a vital role in disease treatment. Sirtuins (SIRTs) are Histone Deacetylase (HDAC) enzyme family members. Seven types of sirtuins (SIRT1–SIRT7) are found throughout cell compartments. They are classified as class III HDACs, and their dependence on Nicotinamide Adenine Dinucleotide (NAD+) as a co-substrate gives rise to the name "NAD+ dependent HDACs [2, 3]. These proteins were initially identified as silencing mating factors due to a characteristic of a sequence in the ancestral yeast gene Silent Information Regulation 2 (Sir2). Sirtuins in mammals are homologues of the yeast Saccharomyces cerevisiae. Sir2 proteins [4]. SIRT1, SIRT6, and SIRT7 are present mostly in the nucleus, whereas SIRT3, SIRT4, and SIRT5 found primarily in the mitochondria [5-7]. SIRT2 is mostly found in the cytoplasm, but it can migrate to the nucleus during mitosis [8]. Sirtuins function in cells through the enzymatic activity of HDAC and/or Adenosine Diphosphate Ribosyltransferase (ADPRT) [9]. Sirtuins have multiple biological functions and have been linked to a variety of diseases, including cancer, metabolic syndrome, and neurological disorders [10]. As sirtuins have been found to be highly expressed in many cancer types, including breast cancer, hepatocellular cancer, prostate cancer, and many others, inhibiting these enzymes appears to be a promising cancer treatment strategy [11]. Sirtinol and salermide are potent and selective naphthalene-based sirtuin inhibitors (Figure 1) [12]. The SIRT1-specific inhibitor of sirtinol inhibited MCF-7 breast cancer cells at an IC50 of 48.6 μ M [13]. Salermide is another example of selective SIRT1 and SIRT2 inhibitor. Salermide inhibits various cancer cells through the induction of apoptosis with an IC50 of 20-100 μ M [14]. In continuation of our work in developing new molecules that tackle epigenetic abnormalities [15-18], we proposed a new naphthalene-based compounds that showed an acceptable virtual binding affinity with SIRT proteins. The designed molecules were synthesized, and their cytotoxicity against breast cancer cells was studied.

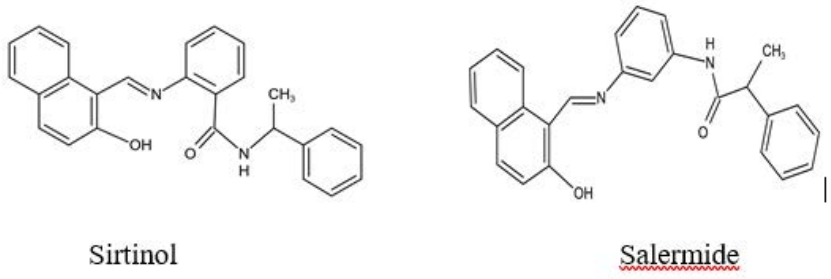

Fig. 1. The chemical structure of representative sirtuin inhibitors

MATERIALS AND METHODS

In Silico study

Protein Preparation and Grid Generation: The crystal structure of homosapien SIRT1-7 proteins was downloaded from the protein data bank (PDB) 4I5I, 5D7P, 4JT8, 5OJN, 2NYR, 6HOY, 5IQZ respectively [19-25]. All the proteins involve NAD in their core as a co-factor and are co-crystalized with a ligand. Proteins were processed using the protein preparation wizard in Schrodinger, New York, NY, 2021, to remove water molecules and non-essential atoms, then the missed atoms in protein residue were added, and finally hydrogen was added, and the hydrogen bonds were optimized by the OLPS_2005 force field. The receptor grid was prepared using the co crystalized ligand as the cener for the boundary box. The dimensions of the boundary box used were 12 A°*12 A°*12 A° [26-27]

Ligand preparation

All ligands were built in chemdraw version 18.0.0.231 and inserted into the prepare ligand module as input files. The ligands energy was minimized using the OLPS_2005 force field in Schrodinger LigPrep software [26].

Molecular docking

The molecular docking experiments were performed using Grid-based Ligand Docking with Energetics (Glide) for receptor-ligand interaction, and ligands were ranked according to the Glide scoring function (G score). The ligands were also evaluated based on potential energy predictions and ligand-binding geometries with SIRT proteins [28]. All compounds docking poses were sorted according to their dock score function and visualized using the Maestro v 13.0.135 interface (Schrodinger, New York, NY, 2021). The extra precision (XP) docking investigation was used to determine the compounds binding poses and binding energies [29].

ADMET study

The compounds were submitted to drug-like property prediction using Lipinski's rule of five and ADMET descriptors calculation in the Schrodinger system using Qikprobe software. Lipinski's rule of five takes into account various molecular features, such as the number of hydrogen bond acceptors and donors. The study's goal is to learn about the primary pharmacokinetic aspects of substances, such as aqueous solubility, intestinal absorption, systemic distribution, metabolism, excretion, and hepatotoxicity, among many other ADMET descriptors [30].

Chemistry

Materials and equipment:

Starting materials and reagents were provided by different commercial suppliers (Thomas Beaker, Macklin, Glenham, and Merck), and they were used without further purification. Silica gel (60 mm-120 mm) for chromatography and TLC (20*20 cm) plates were supplied by Merck, and ethyl-acetate: n-hexane were used as the solvent system. The FT-IR spectroscopy (Shimadzu, Japan) was carried out at the University of Baghdad/College of Pharmacy. The NMR studies were performed using Bruker Avance III 400 MHz and 100 MHz spectrometers at the University of Basra/College of Education for Pure Science. The cytotoxic study was carried out at the Iraqi Centre for Cancer and Medical Genetic Research, Mustansiriyah University.

Organic synthesis

Synthesis of N-(6-bromonaphthalen-2-yl)-4-formylbenzamide (3):

A mixture of 4-formylbenzoic acid 2 (750 mg, 5 mmol) in dichloromethane (DCM) (20 mL) was added to a round-bottom flask and cooled to 0oC. Subsequently, 1-ethyl-3-(3-dimethylaminopropyl) carbodiimide (EDC) (852 mg, 5.5 mmol) and a catalytic amount of hydroxy benzotriazole (HOBt) (67.5 mg, 0.5 mmol) were added, followed by the addition of 6-bromonaphthalene amine 1 (1.11 g, 5 mmol), 4-Dimethylaminopyridin (DMAP) (610 mg, 5 mmol), and N, N-Diisopropylethyl (DIPEA) (0.9 g, 7 mmol). The mixture was stirred continuously at 0°C for two hours, then at room temperature for 18 hours. After the reaction was completed, the solvent was removed, and the crude was transferred into a separatory funnel containing 50 mlL of cooled distilled water, 50 mL of ethyl acetate, 10 mL of 5% hydrochloric acid (HCl), and 10% of sodium bicarbonate ($NaHCO_3$). Following separation, the organic layer was collected, filtered, and dried. To obtain the pure amide product, the filtrate was run through silica gel for

column chromatography with (ethyl acetate: n- hexane) as eluent system to obtain a yellow powder with an 80% yield percent. IR (cm-1): 3251 (N-H), 3066 (Ar-H), 2870 (HC=O), 1693 (Ald C=O), 1643 (Amide C=O), 1518 (Ar C=C), 648 (C- 1.Br) cm-1H NMR (400 MHz, DMSO): δ 10.73 (s, 1H Amide N-H), 10.14 (s, 1H HC=O), 8.52 (d, J=2.0 Hz, 1H), 8.27 – 8.12 (m, 3H), 8.09 (d, J=8.2 Hz, 2H), 7.96 – 7.83 (m, 3H), 7.61 (dd, J=8.7, 2.1 Hz, 1H) (Ar-H). 13C NMR (101 MHz, DMSO-d6): δ 193.40 (Ald C=O), 165.51 (Amide C=O), 140.23, 138.54, 137.55, 132.32, 131.70, 130.22, 129.96, 129.85, 129.83, 128.96, 128.08, 122.41, 118.36, 117.11(Ar-C) [15,31].

General procedure for the synthesis of imine and hydrazone derivatives:

In a round bottom flask, compound 3 (708 mg, 2 mmol) in 10 mL of absolute ethanol and 5 drops of glacial acetic acid were added, then the mixture was mixed with equimolar amounts of various amines (2 mmol), as shown in Table 1, and the mixture was refluxed at 78°C for 14-18 hrs. The completion of the reaction is being observed by TLC with ethyl-acetate: n-hexane as a solvent system. As the mixture cooled to room temperature and was poured into cold water (20 mL), it yielded a precipitate product that was filtered and recrystallized from absolute methanol [32-34]

Tab. 1. The types of amines used and the related product

Amine	Product
Para-aminophenol	(E)-N-(6-bromonaphthalen-2-yl)-4-(((4-hydroxy
	phenyl) imino) methyl) benzamide **(Y1)**
Para-aminobenzamide	(E)-N-(6-bromonaphthalen-2-yl)-4-(((4-carb amoyl phenyl) imino) methyl) benzamide (**Y2**)
Phenyl hydrazine	E)-N-(6-bromonaphthalen-2-yl)-4-((2-phenyl
	hydrazineylidene) methyl) benzamide (**Y3**)
2,4-dinitrophenyl hydrazine	(E)-N-(6- bromonaphthalen-2-yl)-4-((2-(2,4-di-nitro phenyl) hydrazineylidene) methyl) benzamide (**Y4**)

(E)-N-(6-bromonaphthalen-2-yl)-4-(((4-hydroxy phenyl) imino) methyl) benzamide (Y1):

IR (cm^{-1}): 3537 (O-H), 3251 (Amide N-H), 3105 (HC=C), 3074 (Ar-H), 1643 (C=O), 1620 (C=N), 1581, 1543 (Ar-C), 1388 (O-H Bending) cm^{-1}. 1H NMR (400 MHz, DMSO): δ 10.63 (s, 1H Amide N-H), 9.63 (s, 1H O-H), 8.74 (s, 1H HC=N), 8.52 (s, 1H), 8.22 – 8.10 (m, 3H), 8.07 (d, J=8.0 Hz, 2H), 7.97 – 7.91 (m, 2H), 7.91 – 7.83 (m, 2H), 7.70 – 7.57 (m, 1H), 7.29 (d, J=8.2 Hz, 2H), 6.84 (d, J=8.2 Hz, 2H) (Ar-H). 13C NMR (101 MHz, DMSO): δ 165.78 (C=O), 157.21 (C=N), 156.57, 142.65, 139.71, 137.75, 136.81, 132.36, 131.62, 130.11 (d, J=15.9 Hz), 129.81, 128.64 (d, J=7.6 Hz), 128.01, 123.28, 122.50, 118.24, 117.02, 116.26 (Ar-C).

(E)-N-(6-bromonaphthalen-2-yl)-4-(((4-carb amoyl phenyl) imi-no) methyl) benzamide (Y2): IR (cm^{-1}): 3375 (Asy N-H), 3251 (Amide N-H), 3170 (Sym N-H), 3100 (HC=C), 3066 (Ar-H), 1643 (C=O), 1624 (C=N), 1581 (Ar C=C) cm-1. 1H NMR (400 MHz, DMSO): δ 10.68 (s, 1H Amide N-H), 8.78 (s, 1H HC=N), 8.53 (s, 1H), 8.20 – 8.10 (m, 5H), 8.04 – 7.83 (m, 6H), 7.71 – 7.58 (m, 2H) (Ar-H), 7.37 (s, 2H NH2).

(E)-N-(6-bromonaphthalen-2-yl)-4-((2-phenyl hydrazineylidene) methyl) benzamide (Y3):

IR (cm^{-1}): 3298 HN-N), 3263 (Amide N-H), 3105 (HC=N), 1639 (C=O), 1624 (C=N), 1577, 1543 (Ar-C=C) cm^{-1}. 1H NMR (400 MHz, DMSO): δ 10.62 (s, 1H HN-N), 10.53 (s, 1H Amide N-H), 8.52 (s, 1H Ar-H), 8.15 (s, 1H HC=N), 8.06 (d, J=8.0 Hz, 2H), 7.93 (d, J=15.3 Hz, 3H), 7.84 (dd, J=12.4, 8.4 Hz, 3H), 7.63 – 7.56 (m, 1H), 7.26 (t, J=7.6 Hz, 2H), 7.15 (d, J=8.0 Hz, 2H), 6.80 (t, J=7.3 Hz, 1H) (Ar-H). 13C NMR (101 MHz, DMSO-d6): δ 165.89 (C=O), 145.40 (C=N), 139.59, 137.91, 135.65, 133.89, 132.39, 131.55, 130.14, 129.81, 129.76, 129.67, 128.70, 127.95, 125.81, 122.55, 119.72, 118.15, 116.92, 112.72 (Ar-C).

(E)-N-(6-bromonaphthalen-2-yl)-4-((2-(2,4-di-nitrophe-nyl) hydrazineylidene) methyl) benzamide (Y4):

IR (cm^{-1}): 3406 (NH-N), 3282 (Amide N-H), 3079 (HC=N), 3032 (Ar-H), 1666 (C=O), 1612 (C=N), 1581 (Asy NO2), 1531 (Ar C=C),1327 (Sym NO2) cm-1. 1H NMR (400 MHz, DMSO): δ 11.78 (s, 1H HN-N), 10.62 (s, 1H Amide N-H), 8.87 (dd, J=8.2, 2.7 Hz, 1H Ar-H), 8.79 (s, 1H HC=N), 8.52 (d, J=11.7 Hz, 1H), 8.41 (dd, J=9.7, 2.7 Hz, 1H), 8.25 (t, J=7.9 Hz, 1H), 8.20 – 7.82 (m, 8H), 7.61 (dd, J= 8.8, 2.1 Hz, 1H) (Ar-H) (Figure 2).

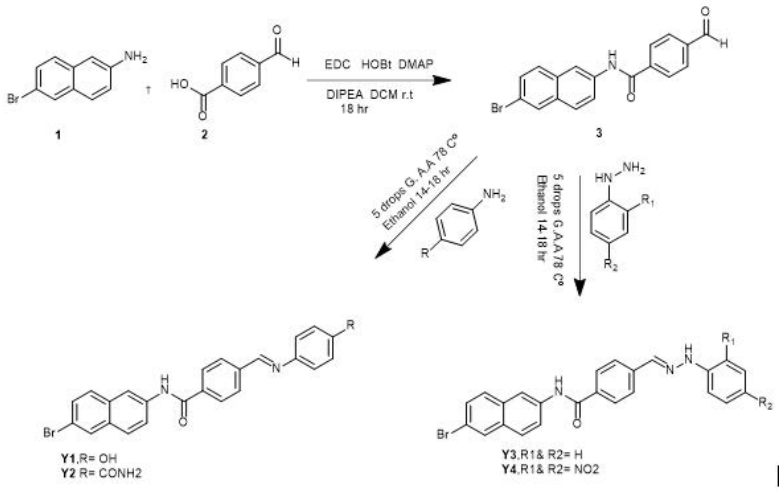

Fig. 2. The organic synthesis for the final compounds

Anti-proliferative study

The final compounds underwent a cancer cell growth inhibition study in comparison with vorinostat. The breast cancer cell line AMJ13 that has been established from an Iraqi patient was used in this study [35]. The stock solution was prepared by dissolving 5 mg of compounds in 1 mL of DMSO to get 5 mg/mL. The stock solution has been filtered by syringe filter paper, and then five dilutions (1 mM, 5 mM, 10 mM, 50 mM, and 100 mM in 200 ml) are prepared using fetal bovine serum 10% (FBS) as a diluent. The dilutions were added to the cells and incubated for 48 hours at 37°C. A control, untreated AMJ13 cell was prepared, as well as a control for the highest concentration of DMSO. The medium of culture was removed when the exposure time was over, then the cell was washed, crystal violet staining solution was added, and it was incubated for 20 minutes. The cell wells were washed to get rid of any extra stain. The optical density of each well at 570 nm (OD570) was measured with a plate reader to compare with the blank and the control of untreated AMJ-13 cells to figure out the percentage of living cells, and then the percentage of inhibition was calculated (36) by using following equation.

$$\% \text{ viability} = (AT - AB) / (AC - AB) \times 100\%$$

Where, AT=Absorbance of treated cells (compounds).
AB=Absorbance of blank (only medium).
AC=Absorbance of control (untreated).
% Inhibition=100–% viability

RESULTS AND DISCUSSION

Docking Study

Generally, all the designed compounds show no significant virtual binding activity for SIRT 1, 2, 3, 7 enzymes. In contrast, the designed compounds exhibited a decent interaction with SIRT 4,5,6. Compound Y4 was highly interacting with SIRT 4,5,6 with acceptable docking scores (Table 1). The virtual interaction of compound Y4 with SIRT4 indicated that the naphthalene moiety was forming a cationic-p interaction with Arg 86 with bond length 5.88 A0 and p-p stacking with Tyr 104 with bond length 3.3 A0. The amide carbonyl group that links the naphthalene moiety with the middle benzene ring forms a hydrogen bond with Ilu 89 with a bond length of 2.6 A0. Most interestingly, the dinitro moieties of Y4 were composing salt bridge interactions with the Arg 103 and Asp 208 residues with bond lengths of 3.4 A0 and 3.8 A0, respectively. These superior virtual interactions between Y4 and SIRT4 might explain the promising antitumor activity of Y4 with breast cancer cells (AMJ14) (Figure 3 and 4) (Table 2).

Tab. 2. Show the XP docking score with sirtuins proteins

Comp No	Docking score (kcal/mol)		
	SIRT4	SIRT5	SIRT6
Comp Y4	-4.35	-5.3	-4.85

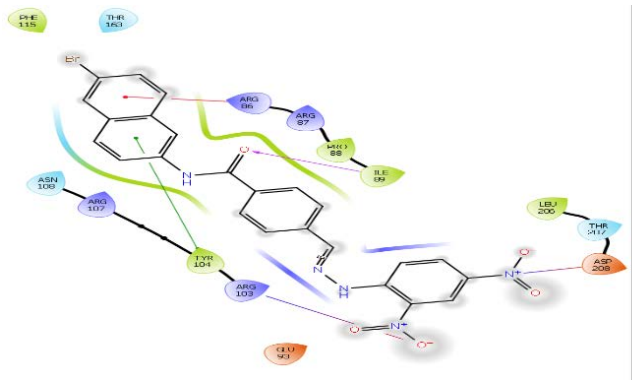

Fig. 3. The 2D interaction of compound Y4 with SIRT4 enzyme

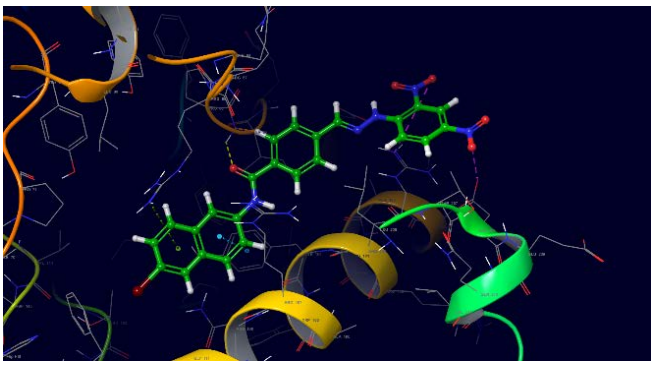

Fig. 4. The 3D interaction of compound Y4 with SIRT4 enzyme

ADMET study

All the compounds obey the Lipinski rule of five and also rule of three of violate Jorgensen's criterion, so all the compounds show an acceptable drug likeness profile as shown in (Table 3).

Tab. 3. Drug likeness properties of proposed compounds

Compound no.	Rule of five	Rule of three	Mw.t g/ mol	TPSA	Clog p	Oral absorption	PCaco	rtvFG
Y1	0	0	444	68.301	4.439	3	932.797	0
Y2	0	0	471	74.67	4.699	3	981.235	0
Y3	0	0	443	57.954	3.57	3	2252.704	0
Y4	1	0	533	145.183	4.279	2	244.065	0

Proposed compounds synthesis

The synthesis of target compounds started with the amide formation reaction between 4-formylbenzoic acid and 6-bromonaphthalene in the presence of EDC, DMAP, HOBt, and DIPEA to form amide 3 (31, 37). The use of EDC instead of DCC for the difficulty of removal of the N, N-dicyclohexylurea by-product rather than the water-soluble EDC by-product. The next step in the formation of an imine bond was carried out by the reaction of the aldehyde group of compound 3 with various amine derivatives in acidic media supported by reflux at 78 oC to obtain the final compounds (Scheme 1) [33].

Cancer cell line study

The breast cancer cells (AMJ-13) used in this study are aggressive, poorly differentiated, and multiply rapidly sice it classified as triple negative breast cancer cell and graded as 3/3 according to Nottingham modification of the Bloom–Richardson system and T2, N0, Mx on TNM staging [35-38]. The observed cells exhibited an elongated multipolar epithelial-like morphology, characterized by nuclear polymorphism and the presence of numerous nuclei in the majority of the cell (Figure 5) [35]. Post-exposure results show inhibition of breast cancer cell growth and lysis of most cells (Figure 5. B, C). Compounds Y1 and Y2 showed moderate antiproliferative activity with a high IC50, while compound Y3 had no activity at the highest concentration of 100 mM. Interest-ingly, compounds Y4 revealed promising cytotoxic activity with an IC50 of (82.8 mM) which is comparable to the FDA-approved HDAC inhibitor vorinostat IC50 of 85.9 mM (Figure 6). A linear regression equation was employed to compute the correlation co-efficient value which is near one so, the inhibition of breast cancer cells is significant (Table 4).

Tab. 4. IC50 values and p-values of vorinostat and the synthesized compounds

Compound	IC_{50}
Vorinostat	85.9 µM
Y1	98 µM
Y2	95.3 µM
Y3	No activity up to 100 µM
Y4	82.8 µM

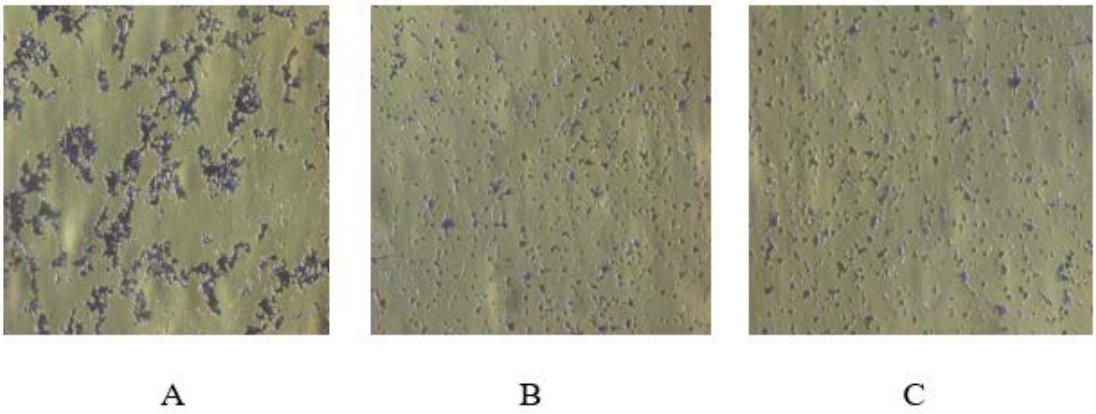

Fig. 5. (A) AMJ13 cancer cell (B) AMJ13 cancer cell treated with Y4 (C) AMJ13 cancer cell treated with vorinostat

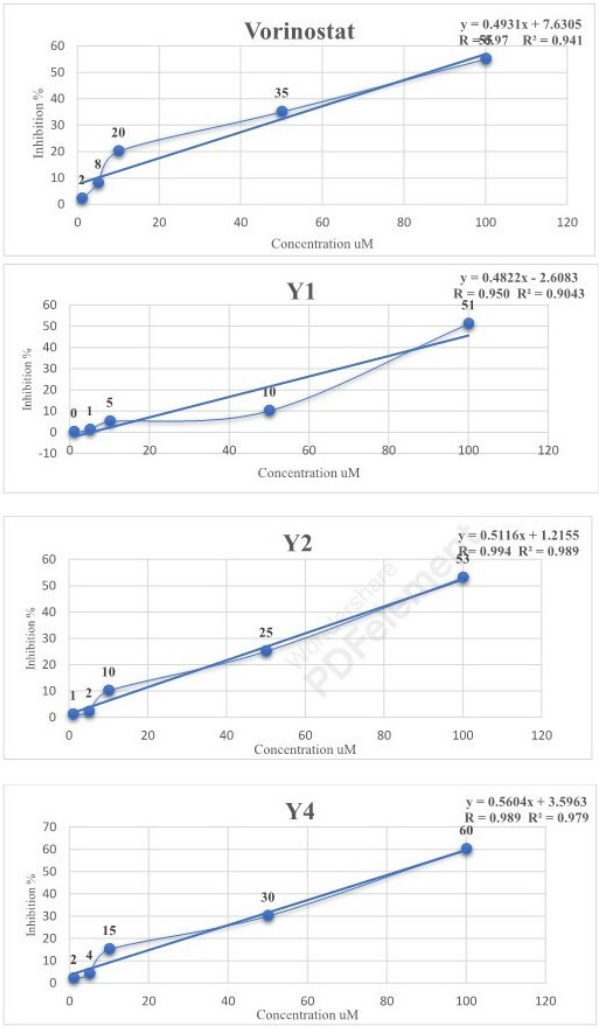

Fig. 6. Plots of the inhibition percent of vorinostat and the synthesized compounds

CONCLUSION

Sirtuin enzymes are prospective therapeutic targets for cancer treatment. New derivatives of the naphthalene moiety were developed using both ligand-based and structure-based drug design. The docking study indicates that the designed molecules bind to SIRT enzymes through various virtual interactions with acceptable docking scores. The final products were successfully synthesized and characterized. The antiproliferative activity against breast cancer cells (AMJ-13) indicates that compound Y4 exhibits a promising inhibition activity that is comparable to the activity of the FDA-approved drug vorinostat. The sirtuin enzymes inhibition activity might be carried out in the future to investigate the potency and selectivity for the synthesized molecules against sirtuins.

DECLARATION OF COMPETING INTEREST

There are no conflicts to declare.

ACKNOWLEDGEMENT

The authors are grateful to the College of Pharmacy, University of Baghdad for its assistance.

REFERENCES

1. Hassanpour SH, Dehghani M. Review of cancer from the perspective of molecular. J Cancer Res Pract. 2017;4:127–129.
2. Teixeira CSS, Cerqueira NMFSA, Gomes P, Sousa SF. A Molecular Perspective on Sirtuin Activity. Int J Mol Sci. 2020;21:8609.
3. Al-Amily D, Mohammed MH. Design, synthesis, and cytotoxicity study of primary amides as histone deacetylase inhibitors. Iraqi J Pharm Sci. 2019 ;28:151–158.
4. Talib LJ, Al-Abbassi MG, Al-Sudani BT. Effect of sirt1 activators on human follicular thyroid cancer. Int J Pharm Res. 2020;12:1608–1620.
5. Sacconnay L, Carrupt PA, Nurisso A. Human sirtuins: Structures and flexibility. J Struct Biol. 2016; 196:534-542.
6. Michishita E, Park JY, Burneskis JM. Evolutionarily conserved and nonconserved cellular localizations and functions of human SIRT proteins. Mol Biol Cell. 2005;16:4623–4635.
7. Onyango P, Celic I, McCaffery JM. SIRT3, a human SIR2 homologue, is an NAD-dependent deacetylase localized to mitochondria. Proc Natl Acad Sci U S A. 2002;99:13653-13658.
8. North BJ, Marshall BL, Borra MT. The Human Sir2 Ortholog, SIRT2, Is an NAD-Dependent Tubulin Deacetylase mouse Sir2 deacetylate the transcription factor protein p53 and suppress p53-dependent apoptosis in re. Mol Cell. 2003;11:437–444.
9. Frye RA. Phylogenetic classification of prokaryotic and eukaryotic Sir2-like proteins. Biochem Biophys Res Commun. 2000;273:793–798.
10. Song J, Yang B, Jia X. Distinctive Roles of Sirtuins on Diabetes, Protective or Detrimental? Front Endocrinol (Lausanne). 2018;9:724.
11. Costa-Machado LF, Fernandez-Marcos PJ. The sirtuin family in cancer. Cell Cycle. 2019;18:2164-2196.
12. Alcaín FJ, Villalba JM. Sirtuin inhibitors. Expert Opin Ther Pat. 2009;19:283-294.
13. Wang J, Kim TH, Ahn MY. Sirtinol, a class III HDAC inhibitor, induces apoptotic and autophagic cell death in MCF-7 human breast cancer cells. Int J Oncol. 2012 ;41:1101–1109.
14. Lara E, Mai A, Calvanese V. Salermide, a Sirtuin inhibitor with a strong cancer-specific proapoptotic effect. Oncogene. 2009 ;28:781–791.
15. Al-Hamashi AA, Koranne R, Dlamini S. A new class of cytotoxic agents targets tubulin and disrupts microtubule dynamics. Bioorg Chem. 2021;116.
16. Al-Hamashi AA, Chen D, Deng Y. Discovery of a potent and dual-selective bisubstrate inhibitor for protein arginine methyltransferase 4/5. Acta Pharm Sin B. 2021;11:2709–2718.
17. Al-Hamashi AA, Abdulhadi SL, Ali RMH. Evaluation of Zinc Chelation Ability for Non-Hydroxamic Organic Moieties. Egypt J Chem. 2023 ;66:215–221.
18. Al-Hamashi AA, Diaz K, Huang R. Non-Histone Arginine Methylation by Protein Arginine Methyltransferases. Curr Protein Pept Sci. 2020 ;21:699–712.
19. Zhao X, Allison D, Condon B. The 2.5 Å crystal structure of the SIRT1 catalytic domain bound to nicotinamide adenine dinucleotide (NAD +) and an indole (EX527 analogue) reveals a novel mechanism of histone deacetylase inhibition. J Med Chem. 2013;56:963–369.
20. Rumpf T, Gerhardt S, Einsle O, Jung M. Seeding for sirtuins: Microseed matrix seeding to obtain crystals of human Sirt3 and Sirt2 suitable for soaking. Acta Crystallogr F Struct Biol Commun. 2015;71:1498–1510.
21. Disch JS, Evindar G, Chiu CH. Discovery of thieno[3,2-d]pyrimidine-6-carboxamides as potent inhibitors of SIRT1, SIRT2, and SIRT3. J Med Chem. 2013;56:3666–3679.
22. Pannek M, Simic Z, Fuszard M. Crystal structures of the mitochondrial deacylase Sirtuin 4 reveal isoform-specific acyl recognition and regulation features. Nat Commun. 2017;8.
23. Schuetz A, Min J, Antoshenko T, et al. Structural Basis of Inhibition of the Human NAD+-Dependent Deacetylase SIRT5 by Suramin. Structure. 2007;15:377–389.
24. You W, Steegborn C. Structural Basis of Sirtuin 6 Inhibition by the Hydroxamate Trichostatin A: Implications for Protein Deacylase Drug Development. J Med Chem. 2018;61:10922–10928.
25. Priyanka A, Solanki V, Parkesh R, Thakur KG. Crystal structure of the N-terminal domain of human SIRT7 reveals a three-helical domain architecture. Proteins. 2016; 84:1558–1563.
26. Madhavi Sastry G, Adzhigirey M, Day T. Protein and ligand preparation: Parameters, protocols, and influence on virtual screening enrichments. J Comput Aided Mol Des. 2013 ;27:221–234.
27. Hasan Y, Al-Hamashi A. Identification of Selisistat Derivatives as SIRT1-3 Inhibitors by in Silico Virtual Screening. Turk Comput Theor Chem. 2023;8:1–11.
28. Friesner RA, Banks JL, Murphy RB. Glide: A New Approach for Rapid, Accurate Docking and Scoring. 1. Method and Assessment of Docking Accuracy. J Med Chem. 2004;47:1739–1749.
29. Friesner RA, Murphy RB, Repasky MP. Extra precision glide: Docking and scoring incorporating a model of hydrophobic enclosure for protein-ligand complexes. J Med Chem. 2006 ;49:6177–6196.
30. Jayapriya, M.; Ali Muhammad, S.; Ravi, S. Synthesis, Anticancer activity, Molecular docking, and Absorption, Distribution, Metabolism, and Excretion toxicity studies of novel benzothiazens. Asian J Pharm Clin Res. 2016;9:61-65.
31. Ghosh AK, Shahabi D. Synthesis of amide derivatives for electron-deficient amines and functionalized carboxylic acids using EDC and DMAP and a catalytic amount of HOBt as the coupling reagents. Tetrahedron Lett. 2021;63:152719.
32. Phadnaik G. A Short Review: Methodologies for the Synthesis of Schiff's Bases. Indian J Adv Chem Sci. 2020; 8: 163-176.
33. Berber N. Preparation and Characterization of Some Schiff Base Compounds. Adıyaman Univ J Sci. 2020; 10: 179-188.
34. Mohammed KH, Nedaa A. Hameed A. Rahim, Ahmed T. Sulaiman. Synthesis, Characterization and Preliminary Antimicrobial Evaluation of New Schiff bases and Aminothiadiazole Derivatives of N-Substituted Phthalimide. Res J Pharm Tech. 2022; 15:3861-3865.
35. Al-Shammari AM, Alshami MA, Umran MA, et al. Establishment and characterization of a receptor-negative, hormone-nonresponsive breast cancer cell line from an Iraqi patient. Breast Cancer: Targets Ther. 2015; 7:223–230.
36. Feoktistova M, Geserick P, Leverkus M. Crystal violet assay for determining the viability of cultured cells. Cold Spring Harb Protoc. 2016 ;2016:343–346.
37. Oleiwi MA, Zalzala MH. Synthesis, Molecular Docking Study and Cytotoxicity Evaluation of some Quinazolinone Derivatives as Nonclassical Antifolates and Potential Cytotoxic Agents. Iraqi J Pharm Sci. 2022;31:283–296.
38. Van Dooijeweert C, van Diest PJ, Ellis IO. Grading of invasive breast carcinoma: the way forward. Virchows Arch. 2022;480:33-43.